

Physics-Guided Actor-Critic Reinforcement Learning for Swimming in Turbulence

Christopher Koh, Laurent Pagnier and Michael (Misha) Chertkov
Applied Mathematics & Mathematics, University of Arizona, Tucson,
AZ 85721

Abstract

Turbulent diffusion causes particles placed in proximity to separate. We investigate the required swimming efforts to maintain a particle close to its passively advected counterpart. We explore optimally balancing these efforts with the intended goal by developing and comparing a novel Physics-Informed Reinforcement Learning (PIRL) strategy with prescribed control (PC) and standard physics-agnostic Reinforcement Learning strategies. Our PIRL scheme, coined the Actor-Physicist, is an adaptation of the Actor-Critic algorithm in which the Neural Network parameterized Critic is replaced with an analytically derived physical heuristic function (the physicist). This strategy is then compared with an analytically computed optimal PC policy derived from a stochastic optimal control formulation and standard physics-agnostic Actor-Critic type algorithms.

1 Introduction

In this manuscript, we consider a particle in a turbulent flow that swims towards its passive partner to maintain proximity. The particle is controlled by a Reinforcement Learning (RL) agent [1], a methodology in Artificial Intelligence (AI) for solving complex decision-making problems. Unlike other AI methods, RL involves an agent learning through interaction with its environment, balancing exploration and exploitation. Exploration involves trying new actions to gain information about the environment (turbulence), while exploitation uses accumulated knowledge to make optimal decisions. This RL decision-making is linked to the Stochastic Optimal Control (SOC) challenge, where the agent maximizes expected reward under environmental uncertainty. In this study, the reward consists of two competing terms: maintaining distance between the agent and its partner, and penalizing the effort required.

Among RL strategies, Actor-Critic (AC) methods [2] combine policy-based actors with reward-based critics. The "actor" suggests actions based on current policy, and the "critic" evaluates these actions, providing feedback to update the policy and reduce learning variance.

Contemporary RL practices use Neural Networks (NNs) for both the actor and critic, enabling the system to learn complex behaviors and decision-making strategies effectively.

1.1 Our Contributions

Standard NN architectures introduce high training costs and produce solutions that are often uninterpretable. Our investigation seeks to enhance policy convergence for the swimmer’s actions by leveraging our understanding of the turbulent environment and the physics governing the swimmer’s displacement. This manuscript explores strategies that integrate physical principles to improve RL outcomes for swimmers in turbulent flows.

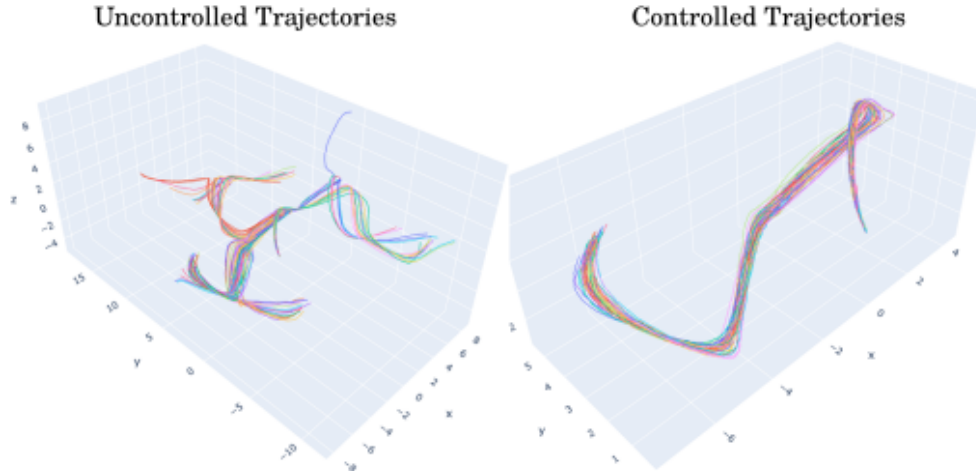


Figure 1: Sample trajectories of passive swimmers/particles (left) placed in a chaotic flow (specifically in the ABC flow, see Section 6.2 for details). Trajectories originating from the same point diverge chaotically along different qualitative trajectories. When under control (right) these trajectories will follow along the trajectory of the single passive particle. These trajectories diverge and fluctuate (see e.g. Fig. (4)a for the separation statistics) but not as violently as without control.

This manuscript’s key technical advancement is the development of a Physics-Informed Reinforcement Learning (PIRL) approach, termed Actor-Critic/Physicist (AC/P), where the Physicist replaces the Critic in the standard Actor-Critic (AC) RL algorithm. The Physicist component leverages physical insights on the statistics and control of swimming in chaotic flows, as elaborated in [3] and further developed here. This approach, derived from our understanding of Lagrangian separation in turbulent flows, guides the control policies. See Section 5.3.1 and Section 5.3.2 for more details on the types of chaotic flows and control/RL algorithms considered in the paper and Figure 2 for illustration of the paper’s main ideas.

The introduced AC/P algorithm incorporates theory of statistical hydrodynamics and the control of Lagrangian separation, thereby enhancing the effectiveness and interpretability of the reinforcement learning process. We specifically focus on three types of chaotic flows: the

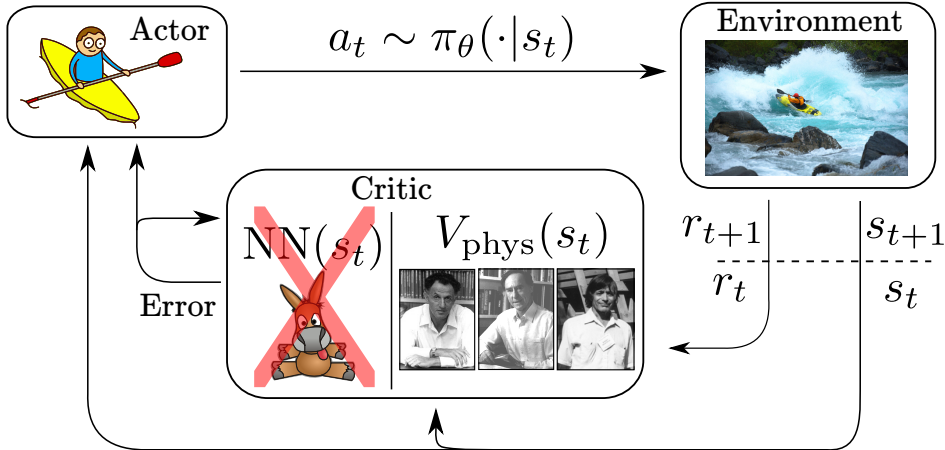


Figure 2: The agent/actor interacts with the environment (turbulence) in the increments, Δ , of time, $t, t \in [0, T]$, where T is duration of the episode. The interaction is expressed via the policy, $\pi_\theta(\text{state}(t))$ where θ are the parameters of a NN representing a probability distribution. Action of the actor ($\phi(t)$) is sampled from the policy. At every iteration in time the acquired reward (which is a known function of the state and the action) is augmented with the information from critic expressed via reward expected for the remaining interval of time within the episode, $t \rightarrow T$. In our physics-informed approach, standard critic (which would be represented by a NN) is replaced by the physics (of turbulence) informed $V_{phys}(\cdot)$. In this work, the derived $V_{phys}(\cdot)$ is parameterized by a single parameter ϕ and is denoted $V_\phi(\cdot)$

Batchelor flow, its Gaussian white-noise counterpart known as the Batchelor-Kraichnan (BK) flow, and the three-dimensional deterministically chaotic Arnold-Beltrami-Childress (ABC) flow, as discussed in Sections 5.3.1, 5.4.1.

Our primary objective is to compare various control policies for the active swimmer, including prescribed control (PC) and standard Actor-Critic RL (AC-RL) methods. By integrating theoretical insights from these models into the AC/P framework, we demonstrate the superiority of the physics-informed approach over conventional RL methods in controlling swimmer dynamics within these complex flow environments. We develop and evaluate several control policies tailored to the available information about flow statistics, detailed in Section 5.3.2 and the rest of the Methods.

2 Problem Setup

In this section, we provide the foundational information necessary for the subsequent analysis, ensuring clarity and self-consistency. We begin by setting up the basic equations for the stochastic dynamics and the statistics of separation between pairs of swimmers, conditioned on a prescribed control (affine in the separation vector and with a fixed rate) in Section 2.1. These expressions will depend on the finite-time statistics of the largest Lyapunov exponent of the chaotic flow (environment), which is also discussed here. Next, we introduce the

Stochastic Optimal Control (SOC) formulation, including the definition of the value function in Section 2.2. Finally, Section 2.3 presents both Basic and Physics-Informed Reinforcement Learning (PIRL) methods, which will be discussed in detail in the following sections.

2.1 Swimming in a Chaotic Flow

We consider a spatially smooth, large-scale chaotic velocity field with a zero mean velocity. This type of flow has been extensively studied in stochastic hydrodynamics (see [4–9], and the relevant review [10]). Particles or swimmers placed in such a flow separate exponentially fast. Our task is to navigate an active swimmer to control its separation from a passive swimmer, assuming they were released in almost the same position initially. Let $\mathbf{s}_\alpha(t) = (s_{\alpha,i}|i = 1, \dots, d)$ represent the positions of the two swimmers, $\alpha = 1, 2$, in d -dimensional flow (where $d = 2$ or $d = 3$). The separation vector $\mathbf{s} = \mathbf{s}_1 - \mathbf{s}_2$ evolves according to:

$$\frac{d\mathbf{s}}{dt} - \mathbf{v}(t, \mathbf{s}_1, \mathbf{s}_2) = -\frac{\mathbf{a}(t) + \boldsymbol{\xi}(t)}{\tau}, \quad (1)$$

where τ is the friction coefficient (set to unity for simplicity), $\mathbf{a}(t) = (a_i(t)|i = 1, \dots, d)$ is the control velocity (thus $\mathbf{a}(t)/\tau$ is the control force) exerted by the active swimmer, and $\boldsymbol{\xi}(t)$ is the difference in thermal forces acting on the active and passive swimmers, modeled as zero-mean white-Gaussian noise:

$$\forall i, j: \quad \mathbb{E}[\xi_i(t)\xi_j(t')] = \kappa_i \delta_{ij} \delta(t - t').$$

The relative velocity vector $\mathbf{v}(t, \mathbf{s}_1, \mathbf{s}_2) = \mathbf{v}_1(t, \mathbf{s}_1) - \mathbf{v}_2(t, \mathbf{s}_2)$ will be modeled differently throughout the manuscript. Following standard stochastic hydrodynamics assumptions [10] for large-scale flows, we approximate $\mathbf{v}(t, \mathbf{s}_1, \mathbf{s}_2)$ by the leading term in its Taylor expansion in \mathbf{s} :

$$\mathbf{v}(t, \mathbf{s}_1, \mathbf{s}_2) \approx \boldsymbol{\sigma}(t)\mathbf{s}, \quad (2)$$

where $\boldsymbol{\sigma}(t)$ is a possibly time-dependent velocity gradient matrix.

We consider two models for $\boldsymbol{\sigma}$ – *general* and *special* in Section 5.4. For the *general* model, we consider an auxiliary multiplicative dynamics:

$$\frac{d}{dt'} \mathbf{W}(t'; t) = \boldsymbol{\sigma}(t') \mathbf{W}(t'; t), \quad (3)$$

where $\mathbf{W}(t'; t) \in \mathbb{R}^{d \times d}$, with $\mathbf{W}(t; t) = \mathbf{1}$, representing the time-ordered exponential of $\boldsymbol{\sigma}(t)$, denoted as $\mathbf{W}(t'; t) = T \exp(\int_t^{t'} dt'' \boldsymbol{\sigma}(t''))$.

2.2 Stochastic Optimal Control and Evaluation of the Value Function

This subsection addresses the formulation and resolution of Stochastic Optimal Control (SOC) problems applied to the swimmer setting. First, we formulate it for a general perspective of large-scale stochastic flow and then focus on the Batchelor-Kraichnan model, which

provides analytical expressions crucial for the data-driven contexts of SOC, such as Reinforcement Learning (RL) [1]. Additionally, we elaborate on different special cases and specifications of SOC, including steady-state (infinite horizon), finite horizon, and those incorporating a discount factor.

We will be working with the value function – also called the expected cost-to-go conditioned on the current state, which we evaluate over a finite horizon from t to T , with the discount factor v :

$$V(t, \mathbf{s}(t)) = \max_{\mathbf{a}(t \rightarrow T)} \left(\int_t^T dt' e^{-v(t'-t)} \mathbb{E} [r(\mathbf{s}(t'); \mathbf{a}(t'))] \right). \quad (4)$$

Here, the expectation is over the stochastic process (large-scale velocity, $\mathbf{v}(t; \mathbf{s})$), and $r(\mathbf{s}(t'); \mathbf{a}(t')) = \|\mathbf{a}(t')\|^2 + \beta \|\mathbf{s}(t')\|^2$ is the reward function dependent on the current state (separation vector between the swimmers), $\mathbf{s}(t')$, and the control (action) vectors, $\mathbf{a}(t')$. Note that the reward is split into two terms – one representing the control efforts (first term) and the other penalizing for larger inter-swimmer distance. Given that without control the swimmers diverge, the two terms are in conflict, and the parameter β allows for a weighting of the separation cost in order to tailor the relative balance of the two terms.

Eq. (4) represents the action-optimized value function. It is also of interest to consider the value function conditioned on the action, specifically when the action is considered in the affine form with respect to the separation vector, $\mathbf{a}(t) \rightarrow \phi \mathbf{s}(t)$, where the rate ϕ is prescribed (fixed to a constant). In the case of a large-scale chaotic flow, this value function conditioned on the control rate ϕ allows the following analytical expression:

$$V(t, \mathbf{s}(t)|\phi) = (\beta + \phi^2) \int_t^T dt' e^{-v(t'-t)} \left(e^{-2\phi(t'-t)} \mathbb{E} [W_{ki}(t'; t) W_{kj}(t'; t)] s_i s_j \right. \\ \left. + \kappa \int_t^{t'} dt'' e^{-2\phi(t'-t'')} \mathbb{E} [\text{Tr} [\mathbf{W}^T(t'; t'') \mathbf{W}(t'; t'')]] \right), \quad (5)$$

where \mathbf{W} satisfies Eq. (3); the expectations are over the statistics of $\boldsymbol{\sigma}$, which is not yet specified, and over the white-Gaussian thermal forces. (We utilize standard Einstein notation, assuming summation over repeated indices.)

As shown in Section 5.5 Eq. (5) for the value function $V(t, \mathbf{s}(t)|\phi)$ allows an analytic estimation, which can then provide the physics guidance for the critic in the AC/P RL algorithm.

2.3 Basic and Physics-Informed Reinforcement Learning

The Stochastic Optimal Control theory discussed in Section 2.2 provides the foundation for Reinforcement Learning (RL) algorithms, enabling us to address the principal practical problem posed and resolved in this manuscript. By adapting the general RL approach, we aim to solve the specific problem of swimmer navigation. This involves setting up a practical framework based on the swimmer's observations of its passive partner and the surrounding flow.

In this manuscript, we complete the description of the problem setup by incorporating these observations, allowing the RL algorithms to effectively guide the swimmer’s navigation.

Pseudo-code for the basic Actor-Critic (AC) algorithm, specifically the Advantage Actor-Critic (A2C) type [11], is provided in Algorithm 1 of the Methods. In our implementation, θ and w represent the neural network parameters for the policy π_θ and the value function V_w , respectively. We run the A2C algorithm over multiple $[0, T]$ episodes, each divided into N steps. At each time step within an episode, these neural networks are updated based on the observed reward given the action taken. Specifically, the networks are updated by evaluating the gradient and taking a step towards the gradient according to the policy gradient and the gradient of the mean squared advantage [1]. This involves updating thousands of parameters for each of the two neural networks at each step.

Our modified Actor-Critic/Physicist (AC/P) algorithm is shown in Algorithm 2 of the Methods. The AC/P algorithm differs from the A2C algorithm in that it replaces the critic (which evaluates the neural network implementation of the value function) with an analytic expression for V_ϕ , detailed in Eq. (16). V_ϕ , representing the physicist/critic, is parameterized by a single fixed parameter ϕ . It is important to note that, while not done in this manuscript, ϕ could be updated similarly to w in the physics-agnostic implementation, which would still be computationally cheaper than updating many more parameters like w . Crucially, the selection of ϕ does not depend on $a(t)$, the action taken, as introducing such dependency would undermine the convergence guarantees of the AC algorithm [1].

3 Results

In this section, we test the AC/P RL algorithm and demonstrate its superiority over the state-of-the-art basic (physics-agnostic) version, as well as compare it to a prescribed control with an optimal (or near-optimal) swimming rate. We approach this in two steps. First, in Section 3.1, we calibrate the AC/P approach using the Batchelor-Kraichnan (BK) model. Then, in Section 3.2, we validate the algorithm’s performance on the ABC flow.

Strategically, we aim to address two main questions. First, how well does our derived theory match our flow environments? Specifically, to what extent does our theory, based on guidance from the Batchelor-Kraichnan model, exhibit discrepancies within ABC flows? Second, how do our trained agents perform compared to the prescribed fixed solutions in both the synthetic (BK) and realistic (ABC) flows?

3.1 Calibration on the Batchelor-Kraichnan Model

We calibrate our experiments using the 2D Batchelor-Kraichnan (BK) flow environment where both the SOC formulation and the value function conditioned on the control rate ϕ are analytically tractable.

First, we verify the consistency of the observed stationary distributions with Eq. (11), as shown in Fig. 3a. Then, we compare the numerically computed average, corresponding to the discounted return in Eq. (4), with the predicted baseline in Eq. (16). The results are presented in Fig. 3c.

Next, we test the AC/P RL setting where the actor is modeled by a NN, while the critic’s estimation of the value function conditioned on ϕ is substituted with its baseline expression from Eq. (16). The results, presented in Figure 3d, show that the trained agent matches or

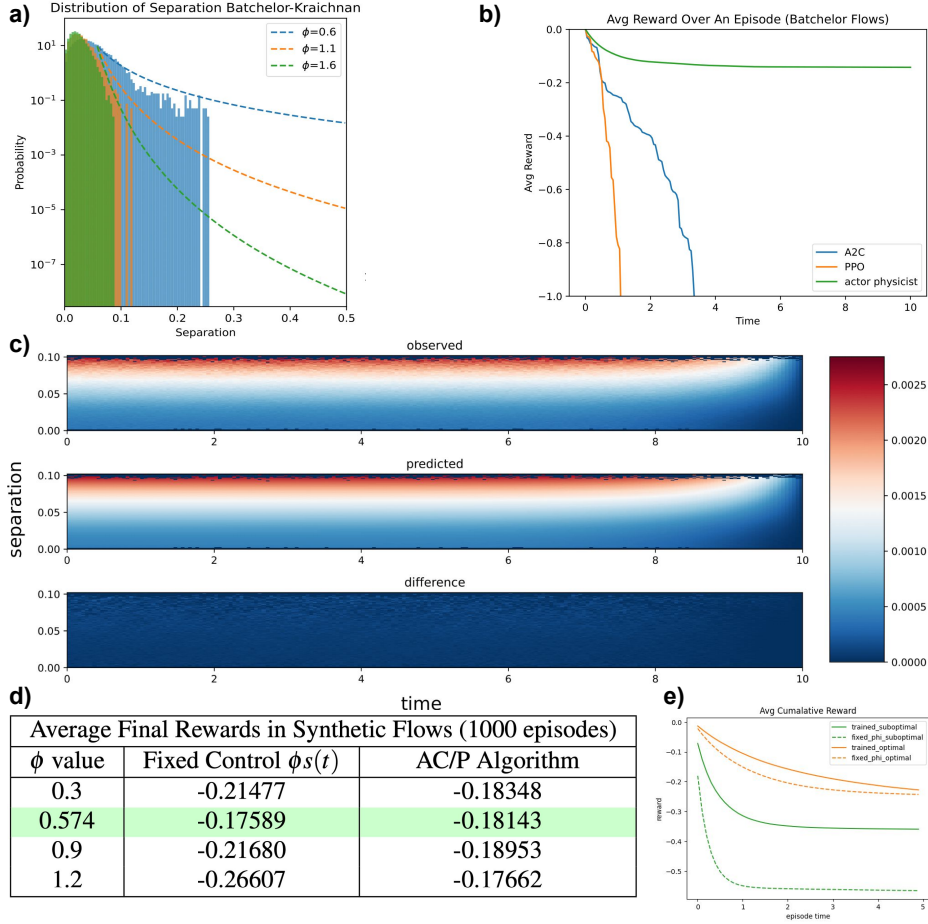


Figure 3: **a)** Log-linear plot of the probability distribution of separation in different ϕ (prescribed control) environments in the BK flows. The dashed lines represent the analytic formula for the BK fit, illustrating a close approximation for the probability distribution in the BK flow. **b)** Average reward over episodes for the physics-informed AC/P algorithm compared to domain-agnostic (physics-uninformed) A2C and PPO. The general-purpose algorithms perform significantly worse compared to the physics-informed algorithm. **c)** Empirical verification of our derived value approximation Eq. (16) in Batchelor flows. The predictions match very closely. **d)** RL-trained baselines nearly always outperform the baseline they were trained on. The exception is when trained on a baseline of 0.574, which is the theory-estimated ϕ^* . (See text for details.) **e)** RL-trained baselines can outperform the optimal ϕ^* for short time episodes (See text for details).

outperforms the corresponding fixed ϕ strategies that their baselines imitate except for the optimal $\phi^0.574$. An interesting result was observed in 3e when training was done over short

episodes. In this case, the trained agent learns to outperform the respective benchmarks corresponding to the optimal ϕ selected according to Eq. (15). This is possible because the optimal ϕ is derived for the stationary regime, achieved asymptotically in the limit of an infinite episode, thus allowing AC/P to outperform it in the short-time regime.

Note that the expression in Eq. (16) for $V(\cdot, \cdot | \phi)$ applies only to cases where the statistics of separation stabilize over time, requiring that $2\phi > \tilde{D}$. Moreover, we expect a critical slowdown effect – when approaching the boundary, i.e., $\phi = \tilde{D}/2 + \varepsilon$ and $\varepsilon \rightarrow 0$, the time required to establish the steady distribution of the separation diverges. This means that, given practical limitations on collecting statistics, Eq. (16) does not apply in the regime of small positive ε , potentially leading to pathological results. (Note that it is important to distinguish between a suboptimal baseline and a pathological baseline. A suboptimal baseline accurately predicts returns following a fixed suboptimal policy, while a pathological baseline does not accurately predict the return and may diverge to infinity or suggest rewarding bad behavior. Agents trained on pathological baselines are likely to exhibit instability in training and poor performance after training.)

3.2 Validation on the ABC Model

We study the ABC flow in the chaotic regime, where trajectories diverge dramatically, largely in an exponential fashion. However, in this case, the Batchelor model, and especially its special Batchelor-Kraichnan case, do not provide an exact match and can only serve as a rough approximation. This is evident in Fig. 4a, which suggests that the statistics of separation observed through simulations and those predicted by matching asymptotic statistics of the leading Lyapunov exponent (matching the Cramér function) and using theoretical predictions for the stationary statistics of separation at different ϕ according to Eq. (11) match only qualitatively. This is not as precise as observed in the BK model test shown in Fig. 3a.

As in the case of the synthetic BK model, our main results concern the AC/P algorithm, where the critic is modeled not via a NN, as in a standard AC approach, but with the baseline Eq. (16) for the value function conditioned on different ϕ . The results, showing the quality of the approximation, are summarized in Figure 4d. We observe that the trained agents tend to match or outperform the corresponding fixed ϕ strategies suggested by the baseline estimation. The one exception is for $\phi = 1.1$, which is notably the value closest to the optimal ϕ^* , estimated by matching the Lyapunov exponent statistics and subsequently using Eq. (15). However, even for $\phi = 1.1$, examination of the distribution of rewards shown in Fig. 4e suggests that the lower value of the experimentally observed average (compared to the respective theory estimate) is due to infrequent large failures linked to atypical/rare events. The figure also shows that the median performance of the trained agent is still better than the median performance of the fixed ϕ agent. This observation implies that for a small number of episodes, the trained AC/P RL agent is most likely to outperform its counterpart following the respective fixed ϕ policy.

In all of our experiments, and especially in the ABC flow experiments, we observe that the physics-informed AC/P RL algorithms significantly outperform the general-purpose AC RL algorithms, such as the Advantage Actor-Critic (A2C) algorithm [11] and the Proximal Policy Optimization (PPO) algorithm [12]. This is particularly evident in Fig. 4e. We attribute this failure of the standard AC RL algorithms to the fact that, although their performance should

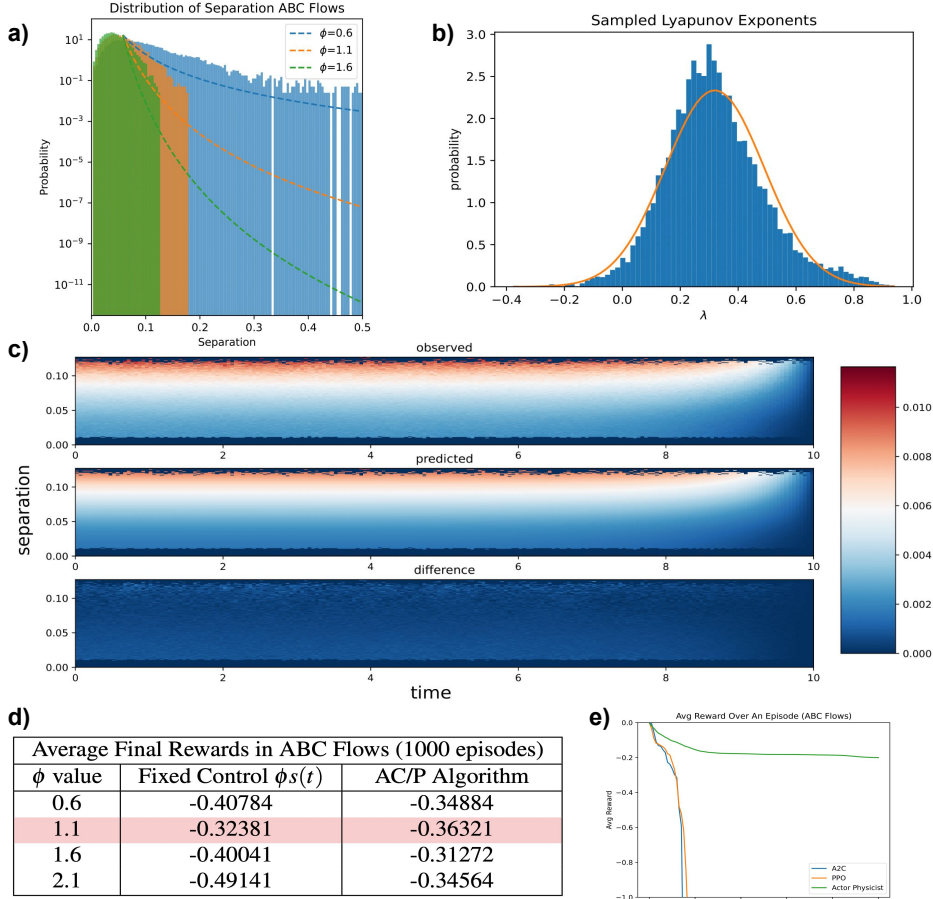
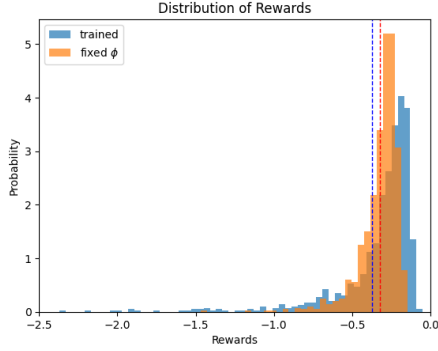


Figure 4: **a)** Log-linear plot of the probability distribution of separation in different ϕ in ABC flows. The dashed lines are the analytic formulas for the BK fit (based on the estimation of $\bar{\lambda}_1$), it is a relatively loose approximation in the ABC flow. **b)** Distribution of sampled λ_1 in the ABC flow (17). The expected value of the leading Lyapunov exponents is used to calculate \bar{D} , subsequently utilized in Eq. (16). **c)** Empirical verification of our derived value approximation Eq. (16) in ABC flows. The predictions match well but the differences between observed and predicted values are larger than in the synthetic environment. **d)** RL-trained baselines nearly always outperform the baseline they were trained on. The exception is when trained on a baseline of 1.1, which is very close to the theory-estimated ϕ^* . (See text for details.) **e)** Average reward over episodes for the physics-informed AC/P algorithm compared to domain-agnostic (physics-uninformed) A2C and PPO. The general-purpose algorithms perform significantly worse compared to the physics-informed algorithm.

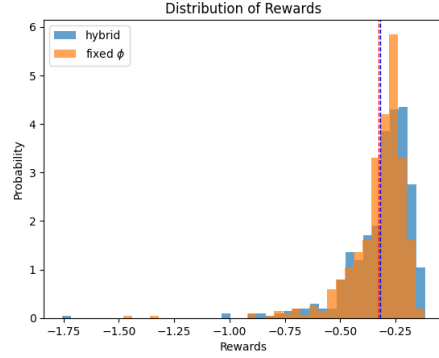
be optimal asymptotically in theory, the actual implementation is never truly asymptotic, especially regarding the number of trials needed for training. This leads to one of the main

conclusions of this manuscript: guiding RL with physics-informed information—specifically, guiding the critic with a theoretical estimate for the value function—makes a significant difference in practical scenarios with finite training resources.

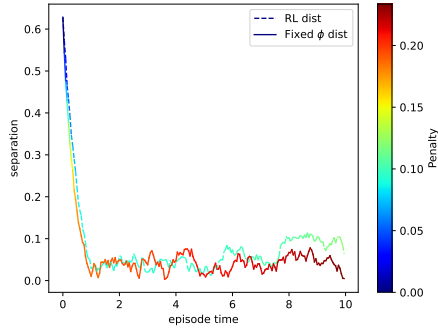
We also hypothesize that the dramatic failure of A2C and PPO may be attributed to the non-standard, fat-tailed statistics in our problem, which show extended algebraic tails, and the large variability in reward values from one configuration of the flow to another, spanning orders of magnitude. These cases are known to be problematic for standard AC RL algorithms [13].



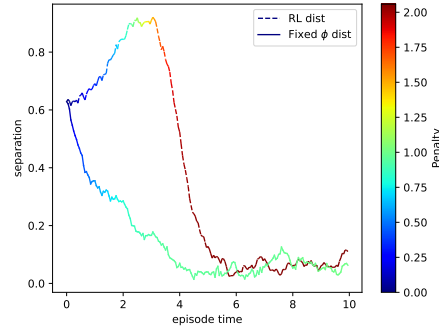
(a) Probability distribution of the final reward in the special case $\phi = 1.1$, the fixed ϕ policy outperforms the AC/P algorithm on average.



(b) Illustrates the performance of the hybrid algorithm, alternating between AC/P and the prescribed ϕ algorithms. See text for details.



(c) Sample trajectory of typical behavior observed in the special case of $\phi = 1.1$, sampled from the illustrated distributions in Fig. 5a



(d) Sample trajectory of atypical behavior observed in the special case of $\phi = 1.1$, sampled from the tails illustrated in Fig. 5a

Figure 5: Analysis of final reward distributions and the accumulated penalty and separation throughout typical and atypical samples. Of note in Fig. 5a the fixed ϕ outperforms AC/P RL agent on average but not in the median value. A hybrid solution in Fig. 5b is able to outperform the fixed ϕ on average and in median value.

Returning to the special case of $\phi = 1.1$, where according to Figure 4d the fixed policy outperforms the AC/P RL, Fig. 5a shows the probability distribution of the final reward accumulated over the entire episode. We observe that the final reward probability distribution indicates that the AC/P RL agent has better median performance but also shows a higher rate of extreme cases (in the tail of the probability distribution) where the AC/P RL algorithm incurs very large penalties. These "bad" cases lead to a significant degradation of the average reward (shown in the figure as the vertical line). Furthermore, the AC/P RL agent exhibits some catastrophic failures—shown as falling off the left side of the figure. Such failures are detectable using the analytic value approximation and can be mitigated via intervention as shown in 5b and expanded upon in the following paragraphs.

To further elaborate on the nuances of typical versus atypical flows, Fig. 5c and 5d shows sample trajectories of the evolution of the separation and the penalty accrued in a typical trajectory versus an atypical trajectory. In the typical case, the AC/P RL agent is much more efficient than the agent following the fixed ϕ policy. In the atypical case, the AC/P RL agent is overly energy conservative and thus converges to the passive swimmer slowly, even showing divergence from the passive partner at the start. In this case, the high penalty is accrued due to the cost of separation. These results imply that the agent could greatly benefit from expanding the state space since it currently has no way to distinguish this episode from the typical case shown on the left in Fig. 5c.

The mention of typical versus atypical behavior in the challenging case where the AC/P RL agent does not perform as well as the fixed ϕ agent helps us draw useful lessons. We learn that a major benefit of a physics-informed baseline is the ability to monitor the trained agent’s performance and identify when the agent may be falling into a regime it cannot handle. In such regimes, intervention with a naive fixed ϕ strategy – that is, designing a hybrid policy that mixes or explores in parallel the RL and fixed ϕ strategies – can avoid catastrophic failures and return the agent to a regime where it outperforms the fixed ϕ policy. Even a simple hybrid solution that switches to the fixed ϕ strategy if the average advantage of the previous n training steps is below a threshold shows improvements. Our results, illustrated in Fig. 5b, show improvements even with arbitrary choices for n and the threshold, suggesting that significant further improvement can be achieved through more principled optimization.

4 Discussions

We study the challenging problem of controlling the separation between a swimmer and its passive partner in chaotic flows using RL. Initially, we observe that state-of-the-art Deep NN-based RL algorithms of the AC type fail at this task due to their inability to handle fat-tail statistics, which exhibit extended power – like/algebraic tails. To address this, we propose a physics-informed approach where the critic utilizes analytic estimations –the average maximum Lyapunov exponent of the flow.

We demonstrate the practicality of the AC/P approach on the Batchelor-Kraichnan flow and validate it on the ABC flow. This approach replaces NN approximations of value functions with physics-of-the-flow-control-informed functions, reducing computational burden and incorporating domain-specific knowledge while maintaining convergence guarantees. Imperfect physics-informed functions can still improve policy training and provide an interpretable measure to identify policy failures, serving as an effective alarm mechanism.

Though focused on a pair of swimmers, this setting can extend to monitoring groups navigating turbulent flows, such as air-drones, flocks of birds, or swarms of aquatic drones. The underlying multi-agent problem reduces to a two-body problem, offering opportunities for future exploration of multi-agent control in turbulent environments. We envision maintaining desired – uniform or stratified – distribution within formations, potentially using mean-field SOC/RL approaches and exploring distributed interactions between temporal neighbors.

Further improvements of the two-particle algorithm include expanding the observed state space to incorporate current separation, history of separation, and local flow information. Additionally, tuning the physics-informed value estimate throughout more elaborate training could improve performance and generalize well to various types of flow.

5 Methods

Our methodology is built on a diverse body of work combining approaches from statistical hydrodynamics, stochastic optimal control and reinforcement learning, therefore we will start the methods section from a brief review of relevant contributions in Section 5.1. Section 5.2 explains the structural relationships between the components of our methodology, including the theoretical framework, RL models, and their application to controlling swimmer separation in chaotic flows. We present a high level description of the chaotic flows and algorithms considered in the paper in Section 5.3. Further details of the Batchelor (general) and then Batchelor-Kraichnan (special) theory explaining statistics of separation of the swimmers without control (first), and then under control are given in Section 5.4.

5.1 Relevant Contributions

Posing the swimmer problem as a Stochastic Optimal Control (SOC) problem, as stated in [3], is appealing because it allows for analytically determining the optimal control. However, this analytical tractability is limited to cases where the stochastic velocity is large scale and either the velocity gradient is δ -correlated in time and Gaussian (Batchelor-Kraichnan model) or, more generally, if the velocity is large-scale (Batchelor type) and the Cramér function (describing the finite time statistics of the leading Lyapunov exponent) is known. In less constrained and more realistic flows, such as the ABC flow used in this paper for validation, the SOC formulation is impractical. In these scenarios, Reinforcement Learning (RL) becomes crucial.

Even though the use of RL in fluid mechanics is relatively recent, a substantial body of work has already accumulated, as reviewed in [14] and [15]. One interesting idea, discussed in [16, 17], is to use multi-agent reinforcement learning with agents distributed over static computational grids to devise novel reduced order models of the Large Eddy Simulation type for complex flows. Multi-agent distributed RL of a mean-field control type was also developed in [18] to control the advancement of a swarm of many Lagrangian swimmers, which do not affect the flow but are tasked with accommodating contrasting requirements, such as staying in a group while avoiding close encounters and limiting energy expenditure for maneuvering.

In another approach, single-agent RL methods were developed for controlling particle (or solid body) navigation specific for efficient gliding in natural stratified air-flow environments [19, 20] and for autonomous navigation along an optimal point-to-point path in various complex fluid flows [21–23]. RL with multiple, or at least two, conflicting objectives was also

extended to a competitive game played by two active swimmers in a turbulent environment, with one attempting to catch and the other aiming to escape [24]. Finally, in a setting closely related to the one discussed in this manuscript, the authors of [25] devised a multi-objective (pareto-seeking) RL approach aimed at controlling separation and minimizing efforts between two active swimmers by switching in time between a number of prescribed strategies, with observations of the separation and velocity difference available at all times. Notably, [21] utilized the Actor-Critic (AC) version of RL, which is central to this manuscript, although their critic is modeled via a neural network in a physics-agnostic (of flow) manner. The RL study in [25] was complemented by a parallel study by the same authors [?], which juxtaposed a stochastic optimal control approach to the problem of a swimmer following a partner in a turbulent flow with a heuristic strategy that relies on the swimmer’s local observation of the environment.

Most of the aforementioned RL papers, with the exceptions of [18, 24, 25], utilize RL in a domain-agnostic, physics-uninformed manner, relying heavily on feature engineering of the underlying neural networks to achieve satisfactory performance. In contrast, our AC/P-RL method encodes domain knowledge through value approximation and does not require enhancements in the modeling of the agents themselves. Additionally, this physics-informed RL approach helps address the difficulties traditional AC methods face in learning values across multiple orders of magnitude [13] and serves as an alternative to jump-start or imitation learning from a warm start [26], which is relevant beyond the context of RL for swimming.

5.2 Integration of Theory and Models in Our Methodology

Our methods’ flowchart is displayed in Fig. 6. On the left-hand side, there are two fundamental elements of Reinforcement Learning: the environment and the agent. In the middle, theory provides a comprehension on which the models can rely. On the right-hand side, we list the models in a hierarchy, from the most interpretable, which rely on strong assumptions that may not be satisfied by the environment, at the top, to the least interpretable, in this case a standard RL agent, at the bottom. Arrows describe the models’ inheritance and how they acquire information about the environment’s physics.

5.3 Chaotic Flows and Algorithm Considered

5.3.1 Chaotic Flows

We analyze three types of chaotic flows:

1. Stochastic large-scale stationary flows, specifically the general position Batchelor flow [4], governed by the flow’s largest Lyapunov exponent [6, 7, 9], see also [10].
2. The short-correlated, Gaussian Batchelor-Kraichnan (BK) flow [5]. (Details are provided in Section 5.4.3.)
3. The three-dimensional Arnold-Beltrami-Childress (ABC) flow [27], illustrated in Fig. (1) for exponential divergence of particle pairs with and without control.

Analytical analysis is feasible for the first two cases, serving as a foundation for experimental validation in the third case (ABC flow). Insights from cases #1 and #2 inform the physics-aware critic, enabling the extension of theory to the AC/P algorithm for more realistic validation in the ABC flow.

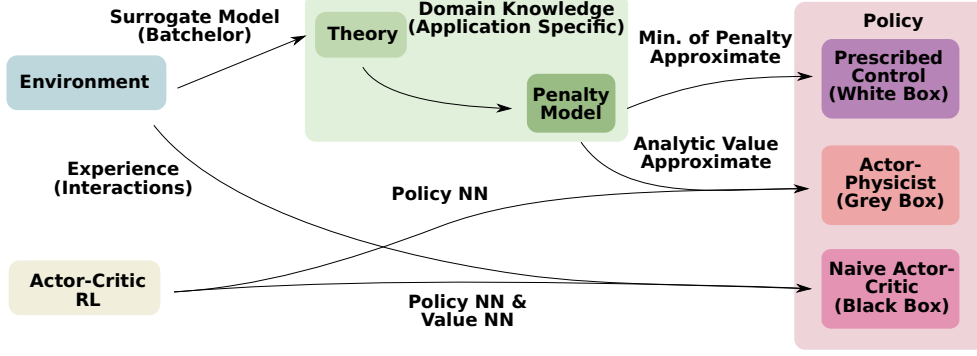


Figure 6: This manuscript discusses and implements various Reinforcement Learning (RL) algorithms in relation to stochastic flow modeling and Stochastic Optimal Control (SOC) theory. The General Batchelor theory, along with a surrogate model based on its Batchelor-Kraichnan (BK) version, is employed to describe the statistics of the separation between pairs of swimmers (both passive and active/controlled by the rate ϕ) in a chaotic flow (see Section 5.4.3 of the Methods). This theoretical framework guides the prescribed control/policy and the Actor-Critic/Physicist (AC/P) RL algorithm. In this context, the physicist (critic) uses BK theory to estimate the value function for SOC, while the control policy in the AC/P approach is approximated by a deep neural network, which is updated based on the approximate value function estimation. Additionally, we compare the prescribed policy and the AC/P approach to the more standard Actor-Critic (AC) approach.

5.3.2 Control and Reinforcement Learning Algorithms

Our primary objective is to maintain proximity between passive and active swimmers by maximizing a time-integrated and averaged reward function. We develop and evaluate several control policies for the active swimmer, tailored to the available information about flow statistics (leading Lyapunov exponent). We compare these policies/controls over discrete time intervals, $[t_k, t_{k+1} = t_k + \Delta]$, $k = 0, \dots$, each of short duration Δ . Depending on the setup, we run either long-term simulations or finite horizon episodes.

- **PC** – Prescribed Control: The control force $\mathbf{a}(t_{k+1}) = \phi \mathbf{s}(t_k)$ is applied based on the separation vector $\mathbf{s}_k = \mathbf{s}(t_k)$ at the previous step. The rate ϕ is fixed, with no RL applied. An analytically optimal ϕ^* can be found for the BK model.
- **AC-RL** – Actor-Critic RL: Standard actor critic type approach where the policy is updated based on the advantage function $A(t_k) = R(\mathbf{s}(t_{k+1}), \mathbf{a}(t_{k+1})) + V(t_k, \mathbf{s}(t_k)) - V(t_{k+1}, \mathbf{s}(t_{k+1}))$, with $V(\cdot, \cdot)$ parameterized by an NN. The policy/actor NN is optimized to maximize the advantage, while the value function/critic NN is updated to accurately predict $V_{NN}(\cdot)$ under the current policy.
- **AC/P-RL** – Actor-Critic/Physicist RL: This method modifies the AC-RL framework by using an analytically derived estimate of the value function $V(\cdot, \cdot | \phi)$ instead of $V_{NN}(\cdot, \cdot)$. This removes the computational cost of updating $V_{NN}(\cdot, \cdot)$ and provides an interpretable measure to gauge policy performance during evaluation. A high-level summary is shown in Figure 2.

5.4 Particle/Swimmer Separation in Large Scale Flows

5.4.1 Batchelor Model of Exponential Divergence

According to the Oseledets theorem [10, 28, 29], at sufficiently large times, the matrix $\log(\mathbf{W}^+(t';t)\mathbf{W}(t';t))/(t'-t)$ stabilizes, with eigenvectors tending to d fixed orthonormal eigenvectors, \mathbf{f}_i , and the eigenvalues $\lambda_i(t';t) = \log|\mathbf{W}(t';t)\mathbf{f}_i|/(t'-t)$ stabilizing to their mean values. The finite-time statistics of λ_i is given by:

$$\text{general: } P(\lambda_1(t';t), \dots, \lambda_d(t';t)|t'-t) \propto \exp(-(t'-t)S(\lambda_1(t';t), \dots, \lambda_d(t';t))), \quad (6)$$

where $S(\cdot)$, called the Cramér function, is convex, and the Lyapunov exponents are ordered: $\lambda_1 \geq \lambda_2 \geq \dots \geq \lambda_d$. Of particular interest are the finite-time statistics of the leading Lyapunov exponent:

$$P(\lambda_1(t';t)|t'-t) \propto \exp(-(t'-t)S_1(\lambda_1(t';t))). \quad (7)$$

This manuscript focuses primarily on the reduced description of the flow associated with the statistics of the relative separation of two swimmers, allowing us to limit our discussion to the finite-time statistics of $\lambda_1(t';t)$. Computing $S_1(\cdot)$ – the Cramér function of $\lambda_1(t';t)$ – analytically is possible only for a limited number of special, idealized flows, such as the stochastic Batchelor-Kraichnan flow [7, 9, 30]. Therefore, our approach to computing $S_1(\lambda_1)$ in large-scale chaotic flows – such as discussed in Section 6.2 for our running example of the ABC flow – will be empirical. We extract it from simulations by placing two particles close to each other initially, tracking their separation over time, and then computing the Cramér function by building statistics of the log-separation divided by time, accumulated over many trials, and fitting it to the expression on the right-hand side of Eq. (7).

5.4.2 Separation in a Batchelor Flow under Control

Consider an active swimmer moving towards its passive counterpart governed by a linear-feedback and time-independent force. This controlled motion can be expressed as

$$\text{Linear Feedback, Time-Independent: } \mathbf{a} \rightarrow \phi \mathbf{s}. \quad (8)$$

Here, ϕ is a constant (time-independent) parameter. Assuming that ϕ is sufficiently large, we focus our analysis on the steady state of the probability distribution function representing distance between the two swimmers. We discuss this scenario under two contexts: first in the general Batchelor case and then in the special short-time correlated case of the Batchelor-Kraichnan model.

In the general Batchelor case solution of Eq. (1) for $\mathbf{s}(t)$ observed at the time t conditioned to $\mathbf{s}(0) = \mathbf{r}_0$, becomes

$$\mathbf{s}(t) = e^{-\phi t} \mathbf{W}(t) \left(\mathbf{s}_0 + \int_0^t dt' e^{\phi t'} \mathbf{W}^{-1}(t') \boldsymbol{\xi}(t') \right), \quad (9)$$

where the time-ordered exponential, $\mathbf{W}(t)$, satisfies Eq. (3). We will study the large time statistics of $s(t) = |\mathbf{s}(t)|$, where the initial separation is forgotten, and thus the first term within the brackets on the right hand side of Eq. (9) can be dropped. Moreover, one can see, following the logic of [9] (see also references therein), that in the long-time regime, where the inter-swimmer separation, $s(t)$ is significantly larger than the so-called diffusive scale, $s_d := \sqrt{\kappa/|\bar{\lambda}_1|}$ and $\lambda_1(t) := \max_i(\lambda_i | i = 1, \dots, d)$ is the largest (finite-time) Lyapunov exponent of the Batchelor flow, the fluctuations of $s(t)$ are mainly due to the Lyapunov exponents, distributed according to Eq. (6). In other words, in this asymptotic we can approximate the inter-swimmer distance by

$$s(t) \approx \exp((\lambda_1(t;0) - \phi)t) s_d. \quad (10)$$

Substituting $\lambda_1(t;0)$, expressed via $s(t)$ according to Eq. (10), into Eq. (7), and expanding $S_1(\cdot)$ in the Taylor Series around $\bar{\lambda}_1$, we arrive at the following asymptotic expression for statistics of $s(t) = |\mathbf{s}(t)|$:

$$\begin{aligned} P(s|t) &\propto \frac{1}{s} \exp\left(-t S_1\left(t^{-1} \log\left(\frac{s}{s_d}\right) + \phi\right)\right) \\ &\rightarrow \frac{1}{s} \exp\left(-t \left(S_1(\bar{\lambda}_1) + \left(\frac{1}{t} \log\left(\frac{s}{s_d}\right) + \phi - \bar{\lambda}_1\right)^2 S_1''(\bar{\lambda}_1)\right)\right) \\ &\rightarrow \Big|_{t \rightarrow \infty; s \gg s_d} P_{st}(s) \propto \frac{1}{s} \left(\frac{s_d}{s}\right)^{2(\phi - \bar{\lambda}_1) S_1''(\bar{\lambda}_1)}. \end{aligned} \quad (11)$$

Notice, that the stationary version of the last line in Eq. (11) settles if $\phi > \bar{\lambda}_1$, and that it is fully consistent with Eq. (14), derived for the short δ -correlated velocity gradient, then $S_1''(\bar{\lambda}_1) = 1/((d-1)D)$ and $\bar{\lambda}_1 = d(d-1)D/2$.

Some observations regarding Eq. (11) are in order:

1. We are motivated to formulate a stochastic optimal control problem guided by the expression (11) for the target probability distribution function and aimed at achieving a predetermined value for ϕ . (While it could align with the model detailed in the next subsection, it could also embody broader paradigms such as risk-sensitive or risk-promotive ones.) This task is addressed in the next Subsection.
2. The right-hand side of Eq. (11) may not be fully applicable, especially when $\phi < \phi_c$. Under such conditions the stationarity is not achieved, leading to an increase in a typical inter-particle distance. In this transient scenario, the right-hand side of Eq. (11) solely depicts the distribution's left tail, peaking at $\log(s/s_d) \sim \sqrt{t}$.
3. It's also worth examining the boundary case when $\phi = \bar{\lambda}_1$. This corresponds to an algebraic growth in inter-particle distance, described as $s \sim t^\alpha$, akin to the Richardson model of turbulence where $\alpha = 2/3$.

5.4.3 The case of the Batchelor-Kraichnan model

Let us also start our analysis with a particular Batchelor-Kraichnan model for the chaotic flow in d -dimensions described by the following pair-correlation function of the velocity gradient

matrix, σ , entering Eq. (1):

$$\forall i, j, k, l = 1, \dots, d : \mathbb{E} [\sigma_{ij}(t)\sigma_{kl}(t')] = D(d+1)\delta(t-t') \left(\delta_{jl}\delta_{ik} - \frac{\delta_{ij}\delta_{kl} + \delta_{jk}\delta_{il}}{d+1} \right), \quad (12)$$

where $\delta(\cdot)$ and δ_{ij} are the δ -function and the Kronecker symbol respectively.

Assuming that ϕ is sufficiently large we derive from the stochastic ODE (1) the following Fokker-Planck (FP) equation for the spherically symmetric probability density of \mathbf{s} : (see [31] for details):

$$\mathcal{L}P(\mathbf{s}|\phi) = 0, \quad \mathcal{L} = s^{1-d} \frac{d}{ds} s^d \left(\phi + \frac{1}{2} \left(D(d-1)s + \frac{\kappa}{s} \right) \frac{d}{ds} \right), \quad (13)$$

where $s = |\mathbf{s}|$; and κ stands for covariance of the thermal noise in Eq. (1). Solution of Eq. (13) is

$$P(\mathbf{s}|\phi) = N^{-1} \left(1 + \frac{(d-1)Dr^2}{\kappa} \right)^{-\phi/(D(d-1))}, \quad N = \left(\frac{\pi\kappa}{(d-1)D} \right)^{d/2} \frac{\Gamma(\phi/(D(d-1)) - d/2)}{d\Gamma(\phi/(D(d-1)))}, \quad (14)$$

where N is the normalization coefficient which guarantees that, $\int_0^\infty \Omega_r dr P(\mathbf{s}|\phi) = 1$, $\Omega_r = (\pi^{d/2}/\Gamma(d/2+1))r^{d-1}$. The solution is valid, i.e. the normalization integral is bounded, if $\phi > (d-1)dD/2$.

5.5 Batchelor-Kraichnan Estimation of the Value Function

Here we will be accessing objects of interest assuming that statistics of the velocity gradient is zero-mean white-Gaussian described by Eq. (12).

5.5.1 Steady State Control. No Discount

Considering the steady state (infinite horizon) and no discount, no finite cost version of Eqs. (4), and utilizing Eq. (14) while also assuming that $\phi > \phi^{(s)} = \tilde{D}/2$, where $\tilde{D} = D(d+2)(d-1)$, we arrive at

$$\phi^* = \arg \min_{\phi} \left((\phi^2 + \beta) \int_0^\infty s^2 P(s|\phi) ds \right) = \arg \min_{\phi} \frac{\phi^2 + \beta}{2\phi - \tilde{D}} = \frac{\tilde{D} + \sqrt{4\beta + \tilde{D}^2}}{2}. \quad (15)$$

5.5.2 Analytic Value Function – Constant Linear Feedback

Let us now present the analytic value function V_ϕ , introduced in Eq. (5) for a generic large-scale (Batchelor) flow, in the particular case of our interest here – the Batchelor-Kraichnan regime. Evaluating expectations in Eq. (5) explicitly – over the Batchelor-Kraichnan σ , described by Eq. (12), and over ξ – we arrive at the following expression for V_ϕ function in the BK model evaluated at the time t , dependent on the observation $\mathbf{s}(t)$ and conditioned

to the fixed value of ϕ :

$$\begin{aligned}
V_\phi(s(t)) &= (\beta + \phi^2) \int_t^T dt' e^{-\nu(t'-t)} \left(s^2 e^{-(2\phi - \bar{D})(t'-t)} + \kappa d \int_t^{t'} dt'' e^{-(2\phi - \bar{D})(t'-t'')} \right) \quad (16) \\
&= A(t)s^2 + B(t), \quad A(t) = \frac{(\beta + \phi^2) \left(1 - e^{-(T-t)(\nu+2\phi - \bar{D})} \right)}{\nu + 2\phi - \bar{D}}, \\
B(t) &= \frac{d\kappa(\beta + \phi^2)}{\nu(2\phi - \bar{D})} \left(1 - e^{-\nu(T-t)} - \frac{\nu(1 - e^{-(T-t)(\nu+2\phi - \bar{D})})}{\nu + 2\phi - \bar{D}} \right),
\end{aligned}$$

where we take into account that within the Batchelor-Kraichnan model $\mathbb{E} [W_{ki}(t';t)W_{kj}(t';t)] = \delta_{ij} \exp(-(t'-t)\bar{D})$, according to Eq. (12).

Some remarks are in order. First, notice that in the infinite horizon, $T \rightarrow \infty$, and then no discount, $\nu \rightarrow \infty$, limits the surviving, B , part of the final expression in Eq. (16), is fully consistent with yet not optimized over ϕ part of the steady expression in Eq. (15). Second, note that even though we emphasize in Eq. (16) the dependence of A and B only on t , the formula actually provides explicit dependence on all other parameters of the Batchelor-Kraichnan flow and of the optimization formulation.

Code Availability

Code is available at https://github.com/Cfckoh/RL_swimmers/tree/main

Data Availability

Data is generated from interactions with the environment and no specific data is needed beyond the code at https://github.com/Cfckoh/RL_swimmers/tree/main.

References

- [1] Sutton, R.S., Barto, A.G.: Reinforcement Learning: an Introduction, Second edition edn. Adaptive computation and machine learning series. The MIT Press, Cambridge, Massachusetts (2018)
- [2] Konda, V., Tsitsiklis, J.: Actor-Critic Algorithms. In: Solla, S., Leen, T., Müller, K. (eds.) Advances in Neural Information Processing Systems, vol. 12. MIT Press, Denver, CO, USA (1999). https://proceedings.neurips.cc/paper_files/paper/1999/file/6449f44a102fde848669bdd9eb6b76fa-Paper.pdf
- [3] Chertkov, M.: Universality and Control of Fat Tails. arXiv. arXiv:2303.09635 [cond-mat, physics:nlin, stat] (2023). <http://arxiv.org/abs/2303.09635> Accessed 2023-04-02
- [4] Batchelor, G.K.: Small-scale variation of convected quantities like temperature in turbulent fluid Part 1. General discussion and the case of small conductivity. Journal of

- Fluid Mechanics **5**(1), 113–133 (1959) <https://doi.org/10.1017/S002211205900009X> .
Publisher: Cambridge University Press
- [5] Kraichnan, R.H.: Small-Scale Structure of a Scalar Field Convected by Turbulence. *Physics of Fluids* **11**(5), 945 (1968) <https://doi.org/10.1063/1.1692063> . Accessed 2023-02-10
- [6] Shraiman, B.I., Siggia, E.D.: Lagrangian path integrals and fluctuations in random flow. *Physical Review E* **49**(4), 2912–2927 (1994) <https://doi.org/10.1103/PhysRevE.49.2912> . Accessed 2023-02-10
- [7] Chertkov, M., Falkovich, G., Kolokolov, I., Lebedev, V.: Statistics of a passive scalar advected by a large-scale two-dimensional velocity field: Analytic solution. *Phys. Rev. E* **51**(6), 5609–5627 (1995) <https://doi.org/10.1103/PhysRevE.51.5609> . Publisher: American Physical Society
- [8] Bernard, D., Gawedzki, K., Kupiainen, A.: Slow Modes in Passive Advection. *Journal of Statistical Physics* **90**(3-4), 519–569 (1998) <https://doi.org/10.1023/A:1023212600779> . Accessed 2023-02-10
- [9] Balkovsky, E., Fouxon, A.: Universal long-time properties of Lagrangian statistics in the Batchelor regime and their application to the passive scalar problem. *Phys. Rev. E* **60**(4), 4164–4174 (1999) <https://doi.org/10.1103/PhysRevE.60.4164> . Publisher: American Physical Society
- [10] Falkovich, G., Gawedzki, K., Vergassola, M.: Particles and fields in fluid turbulence. *Rev. Mod. Phys.* **73**(4), 913–975 (2001) <https://doi.org/10.1103/RevModPhys.73.913> . Publisher: American Physical Society
- [11] Mnih, V., Badia, A.P., Mirza, M., Graves, A., Lillicrap, T., Harley, T., Silver, D., Kavukcuoglu, K.: Asynchronous Methods for Deep Reinforcement Learning. In: Balcan, M.F., Weinberger, K.Q. (eds.) *Proceedings of The 33rd International Conference on Machine Learning*. *Proceedings of Machine Learning Research*, vol. 48, pp. 1928–1937. PMLR, New York, New York, USA (2016). <https://proceedings.mlr.press/v48/mniha16.html>
- [12] Schulman, J., Wolski, F., Dhariwal, P., Radford, A., Klimov, O.: Proximal Policy Optimization Algorithms. *arXiv*. arXiv:1707.06347 [cs] (2017). <http://arxiv.org/abs/1707.06347> Accessed 2024-05-24
- [13] Hasselt, H., Guez, A., Hessel, M., Mnih, V., Silver, D.: Learning values across many orders of magnitude (2016)
- [14] Garnier, P., Viquerat, J., Rabault, J., Larcher, A., Kuhnle, A., Hachem, E.: A review on deep reinforcement learning for fluid mechanics. *Computers & Fluids* **225**, 104973 (2021) <https://doi.org/10.1016/j.compfluid.2021.104973> . Accessed 2023-07-05

- [15] Rabault, J., Ren, F., Zhang, W., Tang, H., Xu, H.: Deep reinforcement learning in fluid mechanics: A promising method for both active flow control and shape optimization. *Journal of Hydrodynamics* **32**(2), 234–246 (2020) <https://doi.org/10.1007/s42241-020-0028-y>
- [16] Novati, G., De Laroussilhe, H.L., Koumoutsakos, P.: Automating turbulence modelling by multi-agent reinforcement learning. *Nature Machine Intelligence* **3**(1), 87–96 (2021) <https://doi.org/10.1038/s42256-020-00272-0> . Accessed 2023-07-05
- [17] Bae, H.J., Koumoutsakos, P.: Scientific multi-agent reinforcement learning for wall-models of turbulent flows. *Nature Communications* **13**(1), 1443 (2022) <https://doi.org/10.1038/s41467-022-28957-7>
- [18] Borra, F., Cencini, M., Celani, A.: Optimal collision avoidance in swarms of active Brownian particles. *Journal of Statistical Mechanics: Theory and Experiment* **2021**(8), 083401 (2021) <https://doi.org/10.1088/1742-5468/ac12c6> . Accessed 2023-07-05
- [19] Reddy, G., Wong-Ng, J., Celani, A., Sejnowski, T.J., Vergassola, M.: Glider soaring via reinforcement learning in the field. *Nature* **562**(7726), 236–239 (2018) <https://doi.org/10.1038/s41586-018-0533-0>
- [20] Novati, G., Mahadevan, L., Koumoutsakos, P.: Controlled gliding and perching through deep-reinforcement-learning. *Phys. Rev. Fluids* **4**(9), 093902 (2019) <https://doi.org/10.1103/PhysRevFluids.4.093902> . Publisher: American Physical Society
- [21] Biferale, L., Bonaccorso, F., Buzzicotti, M., Clark Di Leoni, P., Gustavsson, K.: Zermelo’s problem: Optimal point-to-point navigation in 2D turbulent flows using reinforcement learning. *Chaos: An Interdisciplinary Journal of Nonlinear Science* **29**(10), 103138 (2019) <https://doi.org/10.1063/1.5120370> . Accessed 2024-05-23
- [22] Alageshan, J.K., Verma, A.K., Bec, J., Pandit, R.: Machine learning strategies for path-planning microswimmers in turbulent flows. *Physical Review E* **101**(4), 043110 (2020) <https://doi.org/10.1103/PhysRevE.101.043110> . arXiv:1910.01728 [physics, stat]. Accessed 2023-07-05
- [23] Gunnarson, P., Mandralis, I., Novati, G., Koumoutsakos, P., Dabiri, J.O.: Learning efficient navigation in vortical flow fields. *Nature Communications* **12**(1), 7143 (2021) <https://doi.org/10.1038/s41467-021-27015-y>
- [24] Borra, F., Biferale, L., Cencini, M., Celani, A.: Reinforcement learning for pursuit and evasion of microswimmers at low Reynolds number. *Physical Review Fluids* **7**(2), 023103 (2022) <https://doi.org/10.1103/PhysRevFluids.7.023103> . Accessed 2023-07-05
- [25] Calascibetta, C., Biferale, L., Borra, F., Celani, A., Cencini, M.: Taming Lagrangian chaos with multi-objective reinforcement learning. *The European Physical Journal E*

- 46(3), 9 (2023) <https://doi.org/10.1140/epje/s10189-023-00271-0> . Accessed 2023-07-05
- [26] Uchendu, I., Xiao, T., Lu, Y., Zhu, B., Yan, M., Simon, J., Bennice, M., Fu, C., Ma, C., Jiao, J., Levine, S., Hausman, K.: *Jump-Start Reinforcement Learning* (2023)
- [27] Zhao, X.-H., Kwek, K.-H., Li, J.-B., Huang, K.-L.: Chaotic and Resonant Streamlines in the ABC Flow. *SIAM Journal on Applied Mathematics* **53**(1), 71–77 (1993). Publisher: Society for Industrial and Applied Mathematics. Accessed 2023-05-17
- [28] Ruelle, D.: Ergodic theory of differentiable dynamical systems. *Publications mathématiques de l’IHÉS* **50**(1), 27–58 (1979) <https://doi.org/10.1007/BF02684768> . Accessed 2023-02-10
- [29] Goldhirsch, I., Sulem, P.-L., Orszag, S.A.: Stability and Lyapunov stability of dynamical systems: A differential approach and a numerical method. *Physica D: Nonlinear Phenomena* **27**(3), 311–337 (1987) [https://doi.org/10.1016/0167-2789\(87\)90034-0](https://doi.org/10.1016/0167-2789(87)90034-0) . Accessed 2023-02-10
- [30] Chertkov, M., Gamba, A., Kolokolov, I.: Exact field-theoretical description of passive scalar convection in an N-dimensional long-range velocity field. *Physics Letters A* **192**(5-6), 435–443 (1994) [https://doi.org/10.1016/0375-9601\(94\)90233-X](https://doi.org/10.1016/0375-9601(94)90233-X) . Accessed 2023-02-10
- [31] Chertkov, M.: On how a joint interaction of two innocent partners (smooth advection and linear damping) produces a strong intermittency. *Physics of Fluids* **10**(11), 3017–3019 (1998) <https://doi.org/10.1063/1.869826> . Accessed 2023-02-10

Acknowledgments

We acknowledge R. Ferrando for useful discussion. This work was supported by MC start up funding from the University of Arizona.

6 Supplementary Material

6.1 Actor Critic Algorithms

Algorithm 1 AC-RL

Require: Number of episodes N . Each episode is split into T intervals. Learning rates $\alpha, \beta > 0$. Discount factor $\gamma \in [0, 1]$.
initialize NN for the policy function π_θ (θ is the NN's vector of parameters)
initialize NN for the value function V_w (w is the NN's vector of parameters)
Initialize s_0
for $episode = 1$ **to** N **do**
 for $t = 1$ **to** T **do**
 $a_t \sim \pi_\theta(\cdot|s_t)$
 Take action a_t , observe s_{t+1}, r_t
 $A_t \leftarrow r_t + \gamma V_w(s_{t+1}) - V_w(s_t)$
 $\theta \leftarrow \theta + \frac{\alpha}{t} \sum_{i=0}^t \nabla_\theta \log(\pi_\theta(a_t|s_t)) A_t$
 $w \leftarrow w + \frac{\beta}{t} \nabla_w \sum_{i=0}^t A_i^2$
 end for
end for

Algorithm 2 AC/P-RL

Require: Number of episodes N . Each episode is split into T intervals. Learning rates $\alpha, \beta > 0$. Discount factor $\gamma \in [0, 1]$.
initialize NN for the policy function π_θ (θ is the NN's vector of parameters)
initialize NN for the value function V_w (w is the NN's vector of parameters)
Initialize s_0
for $episode = 1$ **to** N **do**
 for $t = 1$ **to** T **do**
 $a_t \sim \pi_\theta(\cdot|s_t)$
 Take action a_t , observe s_{t+1}, r_t
 $A_t \leftarrow r_t + \gamma V_\phi(s_{t+1}) - V_\phi(s_t)$ ($V_\phi(\cdot)$ is now an analytically derived function)
 $\theta \leftarrow \theta + \frac{\alpha}{t} \sum_{i=0}^t \nabla_\theta \log(\pi_\theta(a_t|s_t)) A_t$
 $w \leftarrow w + \frac{\beta}{t} \nabla_w \sum_{i=0}^t A_i^2$
 end for
end for

6.2 ABC Flow – Implementation Details

The Arnold–Beltrami–Childress (ABC) flow [27] is a three-dimensional incompressible velocity field which is an exact solution of Euler's equation. Its representation in Cartesian

coordinates, augmented with a noise regularization is

$$\begin{aligned}
v_{\alpha,x}(s_\alpha) &= A \sin(s_{\alpha,z}) + C \cos(s_{\alpha,y}) + \xi_{\alpha,x}, & \xi_{\alpha,x} &= \sqrt{\kappa} \frac{dw_x}{dt} \\
v_{\alpha,y}(s_\alpha) &= B \sin(s_{\alpha,x}) + A \cos(s_{\alpha,z}) + \xi_{\alpha,y}, & \xi_{\alpha,y} &= \sqrt{\kappa} \frac{dw_y}{dt} \\
v_{\alpha,z}(s_\alpha) &= C \sin(s_{\alpha,y}) + B \cos(s_{\alpha,x}) + \xi_{\alpha,z}, & \xi_{\alpha,z} &= \sqrt{\kappa} \frac{dw_z}{dt}
\end{aligned} \tag{17}$$

where $\alpha = 1, 2$ is the swimmer index and A, B and C are three parameters and dw_x, dw_y, dw_z are unit variance Wiener processes. With appropriate selection of A, B and C the flows are chaotic so that if a pair of passive swimmers are placed in the flow their separation grows exponentially with time in the $s \ll 2\pi$ regime, as illustrated in Fig. (1). The small regularization parameter κ is introduced to provide an infinitesimal initial separation for a pair of swimmers even if their initial positions coincide.

We choose the ABC flow as a simple example of a fluid flow that can have chaotic trajectories. Moreover, with the proper choice of the A, B, C parameters and as illustrated in Fig. (4b) through the study of the statistics of the leading Lyapunov exponent, $\bar{\lambda}_1$, the flow is approximately of the Batchelor type (in the regime where the inter-swimmer/particle separation is sufficiently small). Specifically, we observe that for $A = 1.$, $B = 0.7$, $C = 0.43$ used in our numerical experiments, Lagrangian separation in the ABC flow is of the BK type introduced in Section 5.4.3. In this case relation between the \tilde{D} parameter, measuring the eddy-diffusivity strength of the BK flow, and the leading Lyapunov exponent is $\tilde{D} = 2\bar{\lambda}_1(1 + 2/d)$.